

Regioselectivity of methyl chlorobenzoate analogues with trimethylstannyl anions by radical nucleophilic substitution: theoretical and experimental study

Juan P. Montañez, Jorge G. Uranga and Ana N. Santiago*

Received (in Gainesville, FL, USA) 12th November 2009, Accepted 18th January 2010

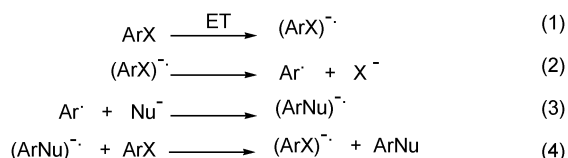
First published as an Advance Article on the web 15th March 2010

DOI: 10.1039/b9nj00664h

Reactions of methyl 2,5-dichlorobenzoate, methyl 4-chlorobenzoate, methyl 2-chlorobenzoate and methyl 3-chlorobenzoate with Me_3Sn^- ions gave the corresponding substitution products by an $\text{S}_{\text{RN}}1$ mechanism. Competition experiments showed that the relative reactivity of chlorine as the leaving group with respect to the ester group in methyl chlorobenzoate is $\text{para} \geq \text{ortho} \gg \text{meta}$ toward Me_3Sn^- ions. Theoretical studies were able to explain the observed reactivity on the basis of the energetic properties of the transition states of the radical anions formed in these reactions.

Introduction

The reaction of triorganostannyl ions as nucleophiles with aryl halides has been studied extensively. The products observed in these reactions depend on the leaving group, the nucleophile, the solvent and on other reaction conditions, but generally occur by halogen–metal exchange (HME) or electron transfer (ET) mechanisms.¹ Photoinitiated ET from the nucleophile is favored among very good electron donor nucleophiles, such as triorganostannyl ions, and also for substrates as aryl halides, which are good electron acceptors. The reaction proceeds through a radical nucleophilic substitution unimolecular mechanism ($\text{S}_{\text{RN}}1$), which is a chain reaction mechanism involving radicals and radical anions (RAs) as intermediates.² The $\text{S}_{\text{RN}}1$ mechanism is shown in Scheme 1.



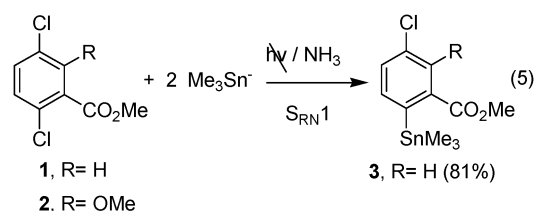
Scheme 1

In the initiation step, an ET from the Nu^- or from a suitable electron source to the substrate takes place, with the radical anion (RA) of the substrate being formed as an intermediate (eqn (1)). This RA cleaves in a subsequent step to form an Ar^{\cdot} radical (eqn (2)). The Ar^{\cdot} radical can then react with Nu^- to give the $\text{ArNu}^{\cdot-}$ radical anion (eqn (3)), which by ET to the substrate forms the intermediates needed to continue the propagation cycle (eqn (4)). The mechanism also involves different termination steps depending on the nature of RX , Nu^- and the experimental conditions. The overall process is a nucleophilic substitution.

The $\text{S}_{\text{RN}}1$ reactions of dihaloarenes with nucleophiles produce either monosubstitution or disubstitution products, depending on the substrate, the nature of the leaving group, the nucleophile and the reaction conditions. For instance, we have previously described the photostimulated reactions of trimethylstannyl ions (Me_3Sn^-) with either methyl 2,5-dichlorobenzoate (**1**) or methyl 3,6-dichloro-2-methoxybenzoate (**2**) in liquid ammonia. These reactions produce $\text{Ar}(\text{SnMe}_3)_2$ with very good to excellent yields (99 and 64%, respectively) by the $\text{S}_{\text{RN}}1$ mechanism.³ However, in dark conditions, **2** yields the reduction product by HME, whereas **1** produces only the monosubstituted product (methylchloro(trimethylstannyl)benzoate; **3**) by the $\text{S}_{\text{RN}}1$ mechanism in 81% yield (eqn (5)) (Scheme 2). In this reaction, two isomers (methyl 5-chloro-2-(trimethylstannyl)benzoate and methyl 2-chloro-5-(trimethylstannyl)benzoate) might be formed. However, only one was observed.⁴

The isomer formed was determined through cleavage of the trimethylstannyl group. This was carried out for methyl chloro(trimethylstannyl)benzoate, which was stirred in concentrated nitric acid at room temperature for 24 h.⁵ The product obtained was identified as methyl *m*-chlorobenzoate by NMR and compared with an authentic sample. This product confirmed the position of chlorine in **3** and the preferred substitution position.

The objective of this paper is to evaluate the relative reactivity of *ortho*-, *meta*- and *para*-chloro-substituted methyl benzoate by the $\text{S}_{\text{RN}}1$ mechanism, in dark and under irradiation conditions. This reactivity was studied experimentally using Me_3Sn^- ions as nucleophiles. In addition, theoretical calculations



Scheme 2

INFIQC, Departamento de Química Orgánica, Facultad de Ciencias Químicas, Universidad Nacional de Córdoba, Ciudad Universitaria, Córdoba 5000 Argentina. E-mail: santiago@fcq.unc.edu.ar; Fax: +54 351 4334170

are also reported to further understand the relative reactivity and the reaction mechanism.

Results and discussion

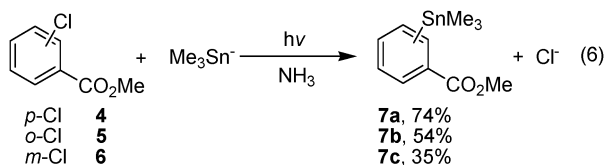
Reactivity of methyl chlorobenzoate

Methyl 4-chlorobenzoate (**4**) and Me_3Sn^- ions reacted in the dark, giving methyl 4-(trimethylstannyl)benzoate (**7a**; 32%) in liquid ammonia. This reaction was catalyzed by light (eqn (6); Scheme 3) and inhibited by well known inhibitors of $\text{S}_{\text{RN}}1$ reactions² (Table 1, expts. 1–4).

In the same way, methyl 2-chlorobenzoate (**5**) and Me_3Sn^- ions reacted in the dark or under photostimulation, producing methyl 2-(trimethylstannyl)benzoate (**7b**; 24 and 54%, respectively) in liquid ammonia (Table 1, expts. 5–6) (eqn (6)). By way of contrast, methyl 3-chlorobenzoate (**6**) failed to react with Me_3Sn^- ions in liquid ammonia in the dark. However, it reacted under photostimulation to give 35% methyl 3-(trimethylstannyl) benzoate (**7c**) (Table 1, expts. 7 and 8). In the absence of the nucleophile (Me_3Sn^-) methyl chlorobenzoates reacted in the dark to produce chlorobenzamide (40–50%) in liquid ammonia. This product, however, was not observed in the presence of the nucleophile.

The fact that these reactions are catalyzed by light, that the substitution products are formed and that the photostimulated reactions are inhibited by well-known radical scavengers suggests that these reactions occur by the $\text{S}_{\text{RN}}1$ mechanism, as shown in Scheme 4. When methyl chlorobenzoate receives one electron, a π -RA, $\mathbf{8}^{\bullet-}$, is formed (eqn (7)). This RA gives radical $\mathbf{9}^{\bullet}$ by fragmentation of the C–Cl bond (eqn (8)), which by reaction with the nucleophile gives a new RA, $\mathbf{10}^{\bullet-}$ (eqn (9)). This intermediate finally affords the substitution products and $\mathbf{8}^{\bullet-}$ (eqn (10)), which can continue the chain propagation steps.

Very low yields of the reduction product (methyl benzoate) were found, indicating that when radical $\mathbf{9}^{\bullet}$ is formed, the



Scheme 3

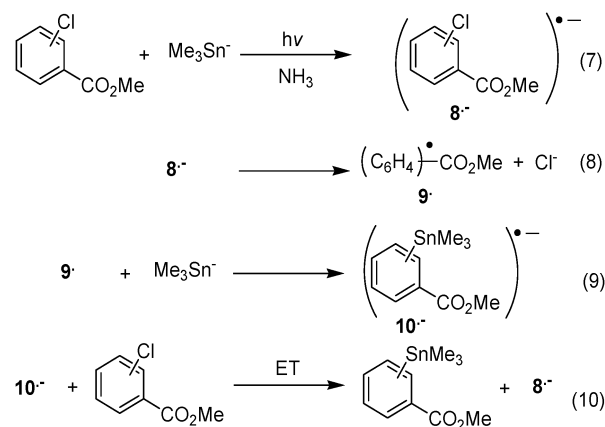
coupling with the nucleophile is faster than the reduction by the solvent.

Relative reactivity of –Cl in *ortho*-, *meta*- and *para*-positions with respect to the ester group

To compare the reactivity of these compounds, their relative reactivity was studied by competition experiments.⁶ In these experiments, the relative reactivity depended on the rate of ET from any of the substitution product RA intermediates to the substrates. From these competition reactions, **4** was 1.16 times more reactive than **5** toward Me_3Sn^- ions in the dark (Table 2, expts. 1–3). In the same way, the dark relative reactivity of **5** was much higher than that of **6** (Table 2, expts. 4 and 5). In photostimulated reactions, the relative reactivity of **5** was 19.3 times higher than that of **6** toward Me_3Sn^- ions (Table 2, expt. 6).

As seen in Table 2, we found that the relative reactivity of the methyl chlorobenzoate isomers was *para* \geq *ortho* \gg *meta*. These results are in agreement with data reported on similar compounds. Tanner *et al.* found that the rate constant for the fragmentation of haloacetophenone RAs was greater for *para*- and *ortho*- compared to *meta*-isomers.⁷ For example, they found that cleavage of the *m*-chloroacetophenone RA was observed to be >20 times slower than that of its *para*-isomer.

These experimental results may explain the reactivity found with substrate **1** under the same conditions. In the dark reaction of **1** with Me_3Sn^- ions, two isomers might be formed:



Scheme 4

Table 1 Reactions of methyl chlorobenzoates with Me_3Sn^- ions in liquid ammonia

Expt.	Substrate, $\text{M} \times 10^{-3}$	Nucleophile $\text{M} \times 10^{-3}$	Conditions (min)	Yields of product, ^a (substrate recovered) ^b
1	4 , 4.0	4.0	NH_3 , dark (60)	7a , 32 (61)
2	4 , 4.0	4.0	NH_3 , $h\nu$ (60)	7a , 74 (—)
3	4 , 4.0	4.0	NH_3 , dark (60) ^c	7a , 21 (48) ^d
4	4 , 4.0	4.0	NH_3 , dark (60) ^e	7a , — (88)
5	5 , 4.0	4.0	NH_3 , dark (60)	7b , 24 (66)
6	5 , 4.0	4.0	NH_3 , $h\nu$ (60)	7b , 54 ^f (18)
7	6 , 4.0	4.0	NH_3 , dark (60)	7c , — (100)
8	6 , 4.0	4.0	NH_3 , $h\nu$ (60)	7c , 35 ^g (34)

^a Quantified by GLC and the internal standard method, with *p*-dibromobenzene as a reference. ^b Recovered and quantified as acid. ^c With 10% *p*-DNB added. ^d Together with 20% substrate recovered as ester. ^e Di-*tert*-butyl nitroxide (17 mol%) was added. ^f Together with 5% methyl benzoate. ^g Together with 10% methyl benzoate.

Table 2 Competition experiments of **4** vs. **5** and **5** vs. **6** with Me_3Sn^- ions^a

Expt.	Substrates, $\text{M} \times 10^{-3}$		$\text{Me}_3\text{Sn}^- \text{M} \times 10^{-3}$	Yield of products (%) ^a		Relation
	4	5		7a	7b	
1 ^b	4 , 4.0	5 , 4.0	4.0	23	19	1.24
2 ^b	4 , 4.0	5 , 4.0	4.0	35	33	1.09
3 ^b	4 , 4.0	5 , 4.0	4.0	21	19	1.12
				$k_4/k_5 = 1.16 \pm 0.08$ (average)		
				7b	7c	
4 ^b	5 , 4.0	6 , 4.0	4.0	49	—	$k_5 \gg k_6$
5 ^b	5 , 4.0	6 , 4.0	4.0	54	—	$k_5 \gg k_6$
6 ^c	5 , 4.0	6 , 4.0	4.0	80	8	$k_5/k_6 = 19.3$

^a The relation quantified by GLC and the internal standard method, with *p*-dibromobenzene as the reference and considering the concentration of the substitution product formed ($[\text{substrate}]_t = [\text{substrate}]_0 - [\text{substitution product}]$) (the relative reactivity of **4** vs. **5** was not calculated under irradiation since reduction product (methyl benzoate) was formed). ^b In the dark for 60 min. ^c Irradiation time 60 min.

3 (*ortho*-substitution) or methyl 2-chloro-5-(trimethylstannyl)benzoate (*meta*-substitution); however only **3** was produced in 81% yield.⁴ This product was formed due to the *ortho*-substitution being much faster than the *meta*-substitution. In other words, the intramolecular ET (intra-ET) to chlorine in the *ortho*-position was faster than the intra-ET to chlorine in the *meta*-position.

Geometric and stereoelectronic parameters

To further understand the experimental results, we also carried out theoretical calculations by employing the B3LYP functional at the 6-31+G* level. Optimized geometries for RAs **1**, **4**, **5** and **6** (Fig. 1A) were obtained. Compounds **5**^{•-} and **1**^{•-} showed an in-plane distortion from the optimal sp^2 $\text{Cl}-\text{C}_2-\text{C}_1$ angle (120°) that is not typical of *ortho*-substituted radical anions. These angles are 122.5 and 122.6° respectively, most certainly due to steric repulsion with the ester group. This distortion could facilitate the fragmentation of the *ortho* position and, to our knowledge, has never been observed in other haloaromatic RAs. Pierini *et al.* demonstrated that out of plane distortions of geometry favoured the cleavage of *ortho*-substituted haloaromatic RAs.^{8,9} However, the repulsive interaction previously reported (out of plane) is quite different from those observed here (in-plane).

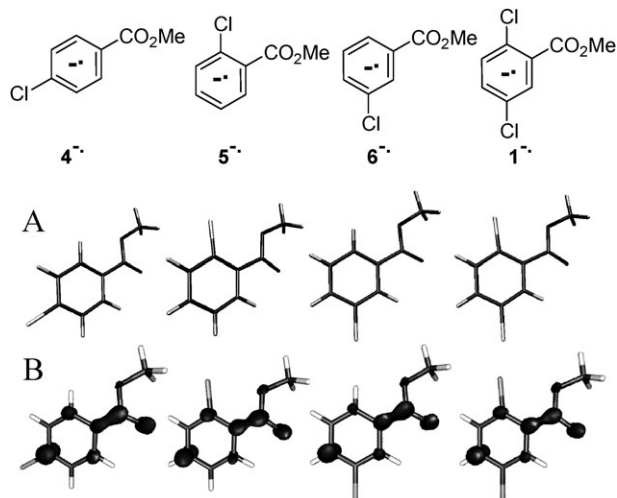


Fig. 1 Geometry and unpaired spin distribution of radical anions **1**, **4**, **5** and **6**.

The spin distribution calculated can also give an indication of a more facile dissociation for RA intermediates. It has been shown that the nodal properties of the MO that hosts the unpaired electron and the spin density distribution are relevant factors for the cleavage of RAs.¹⁰ The spin density of RAs **1**, **4**, **5** and **6** is shown in Fig. 1B. It is easy to see that the ester group determines the spin distribution for the whole family of compounds, which is always higher in its *para*-position, with a nodal spin density at its *meta*-positions. These spin density distributions indicate that the cleavage of RAs could be facilitated in the *ortho*- and *para*-derivates.

The potential energy surfaces (PES) evaluated for the dissociation of RAs of **4–6** are presented in Fig. 2. To our knowledge, this is the first time that it has been possible to locate the transition states for the intra-ET in these compounds. We also found and characterized the corresponding σ^* RA minima as well, which were not reported in previous studies.¹⁰ As can be clearly seen in Fig. 2 and Table 3, the *ortho*- and *para*-isomers have comparable activation barriers for the intra-ET. However, the relative stability of the σ RAs are clearly different, with the *ortho*-substituted compound (**5**) showing similar stability for the σ and π RAs, whereas for compound **4**, the π RA is the more stable.

The energies, geometries and thermodynamic parameters evaluated for the RA intermediates in these reactions are shown in Table 3. The methyl chlorobenzoates (**4–6**) presented in the table had similar electron affinities, thus making their single-electron reduction equally feasible. However, as shown in Table 3, similar activation energies for the intra-ET processes were found for **4** ($3.97 \text{ kcal mol}^{-1}$), **5** ($3.30 \text{ kcal mol}^{-1}$) and **1** (in C_2 , $4.63 \text{ kcal mol}^{-1}$), whereas much larger activation energies for **6** ($10.22 \text{ kcal mol}^{-1}$) and **1** (in C_5 , $10.64 \text{ kcal mol}^{-1}$) were obtained, suggesting that the *meta* fragmentation is slower, in excellent agreement with the experiments. Alternatively, **6**^{•-} has the lowest spin density at C_{ipso} (the carbon bonded to Cl) on its leaving group and is also the isomer showing the largest activation energy. Consequently, one could use the spin distribution to predict the relative reactivity of the isomers.

The difference in energy between the π and σ states ($\Delta E_{\pi\sigma}$) in the RAs is also shown in Table 3. As can be seen, this energy difference is not a good indicator of reactivity since it would predict the *ortho* to be the most reactive isomer. As a result, we propose that this parameter cannot be used to determine the

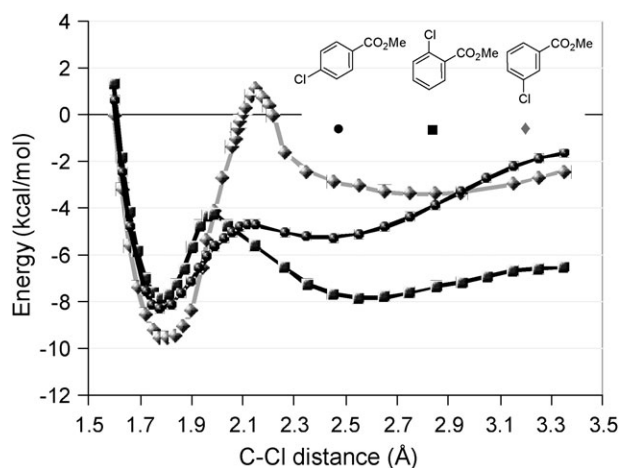


Fig. 2 UB3LYP/6-31+G* gas phase anionic profiles of methyl chlorobenzoates **4***–**6***. The neutral molecules were taken as zero energy.

reactivity order in this type of compound, as proposed previously.⁹

In addition, the solvent's effect was evaluated by single point calculations using acetonitrile as the solvent by means of Tomasi's polarizable continuum model implemented in Gaussian (IEFPCM) (Table 4).¹¹ When the solvent was included, the stabilization of the σ species increased, making the intra-ET for all compounds substantially more exothermic. In addition, including the condensed phase effect, the σ RAs disappeared, *i.e.* the minimum vanished and the potential energy surface became repulsive. The activation energies predict a reactivity order in solution of *para* \geq *ortho* \gg *meta*, as can be seen in Table 4, which is in full agreement with the experimental trend.

The intra-ET profiles for the fragmentation of **1** in the gas phase are presented in Fig. 3. The figure shows the anionic profiles for the two possible fragmentations (*ortho* and *meta*) of the π RA $\mathbf{1}^{\bullet-}$ and the orbital nature of these intermediates, represented as their SOMOs. The PES topologies of **1** for the two possible fragmentations are similar to the above-mentioned ones for **5** and **6**. These results show that the *ortho* fragmentation has substantially lower activation energy than the *meta* fragmentation, which is in excellent agreement with the experiments.

Fig. 4B shows the electrostatic potential at the π RA $\mathbf{1}^{\bullet-}$ and the π - σ^* crossing zone (transition state) for the *ortho* and

Table 4 Thermodynamic and kinetic parameters of the anionic surface with solvent^a

IEFPCM		E^\ddagger	ΔE_{frag}^b	$-EA^c$
1	C ₂	3.30	-1.53	-56.49
	C ₅	8.85	-9.03	
4		1.51	-1.40	-51.27
5		2.38	-2.01	-51.84
6		7.45	-1.31	-52.50

^a Solution phase calculation with acetonitrile as the solvent. ^b ΔE_{frag} (RX \rightarrow R $^\bullet$ + X $^-$) in kcal mol $^{-1}$. ^c ΔE (RX \rightarrow RX $^{\bullet-}$) in kcal mol $^{-1}$.

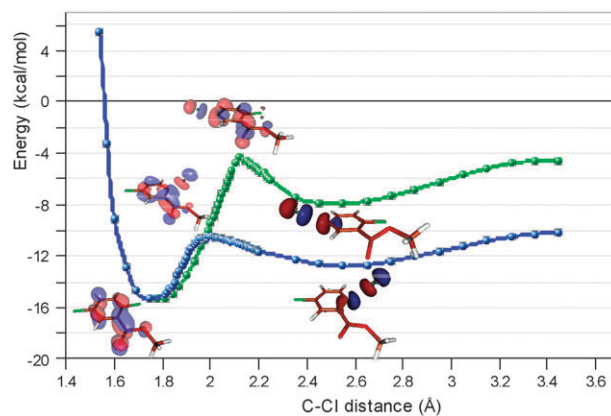


Fig. 3 UB3LYP/6-31+G* anionic profiles for compound **1** (blue = fragmentation in the *ortho*-position, green = fragmentation in the *meta*-position). In all cases, zero energy corresponds to the neutral compounds.

meta fragmentations; Fig. 4A shows the spin density. As can be seen from the molecular electrostatic potential (MEP), the initial π RA has a negative charge on the ester group, with it gradually transferring to the Cl atom in the transition states. A similar behavior was observed for the spin densities, where the σ radical character was formed at the transition state's geometry. For the *ortho* fragmentation it is possible to visualize the larger electrostatic repulsion between the chlorine atom and the ester oxygen, denoted as the red zone in that region of the MEP. On the other hand, this repulsive effect triggered a bigger distortion from planarity at the transition state geometry than that observed in the *meta* isomer.

Table 3 The main geometric, thermodynamic and kinetic parameters of radicals and RA intermediates^a

Compound	π RA		TS		σ^* RA		$\Delta E_{\pi\sigma}$	E^\ddagger	ΔE_{frag}^b	$-EA^c$	
		Cl-C ^d	Angle ^e	Cl-C ^d	Angle ^e	Cl-C ^d					Angle ^e
1	C ₂	1.786	180	2.031	138.95	2.531	137.43	3.13	4.63	131.28	-15.37
	C ₅	1.793	180	2.107	149.18	2.585	155.32	7.79	10.64	136.81	
4		1.784	180	2.140	138.75	2.519	145.46	3.64	3.97	131.25	-8.34
5		1.796	180	1.997	141.08	2.631	139.84	0.57	3.30	124.29	-7.87
6		1.800	180	2.149	154.35	2.691	179.76	6.59	10.22	131.87	-9.56

^a The zero-point energy corrections were made at the 6-31+G* level. In all cases, zero energy corresponded to the neutral compounds. ^b ΔE_{frag} (RX \rightarrow R $^\bullet$ + X $^-$) in kcal mol $^{-1}$. ^c EA (adiabatic electron affinity) ΔE (RX \rightarrow RX $^{\bullet-}$) in kcal mol $^{-1}$. ^d Distance Cl-C_{ipso} in Å. ^e Dihedral angle Cl-C_{ipso}-C $_{\alpha}$ -C $_{\alpha}'$ in degrees, where C $_{\alpha}$ and C $_{\alpha}'$ are neighbours of C_{ipso}.

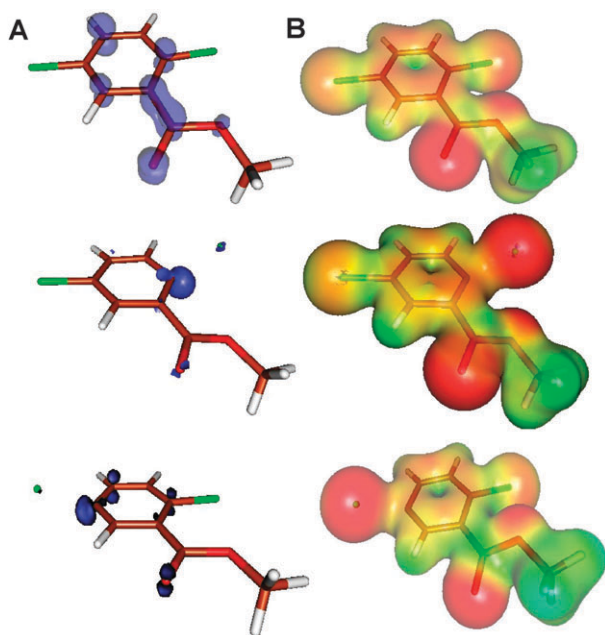


Fig. 4 Spin density (A) and electrostatic potential (B) (from blue = positive to red = negative) on $1^{\bullet+}$ or the indicated points along the reaction path for the *ortho* and *meta* fragmentations.

3. Conclusions

We reported the reactivity and theoretical calculations of methyl chlorobenzoates (*para*, *ortho* and *meta*) and methyl 2,5-dichlorobenzoate with Me_3Sn^- ions through a $\text{S}_{\text{RN}}1$ reaction mechanism. In these conditions, the compounds gave the corresponding substitution product and the reactions were catalyzed by irradiation. The relative reactivity of chlorine as the leaving group with respect to the ester group in methyl chlorobenzoates was *para* \geq *ortho* \gg *meta*. Based on calculations including solvents effects, the activation energies obtained for the fragmentation process reproduce the observed experimental reactivity trend.

4. Experimental

General methods

Irradiation was conducted in a reactor equipped with two 400 W UV lamps emitting maximally at 350 nm (Philips Model HPT, water-refrigerated). The HRMS were recorded at UCR Mass Spectrometry Facility, University of California, United States.

Materials

Methyl 2,5-dichlorobenzoate (**1**), 4-chlorobenzoic acid, 2-chlorobenzoic acid, methyl 3-chlorobenzoate (**6**) and Me_3SnCl were commercially available and used as received. Liquid ammonia was distilled under nitrogen and metallic Na, and used immediately.

Typical procedure for reactions of esterification. preparation of methyl 2-chlorobenzoate (**5**)

The following procedure is representative of these reactions. 2-Chlorobenzoic acid (1 g, 6.4 mmol) was added to 0.71 g,

6.4 mmol of *t*-BuOK dissolved in 25 mL of dry DMSO. Then, the reaction was quenched with 1.14 mL, 6.4 mmol of methyl iodide. The solution was dissolved with water and then extracted with diethyl ether. Methyl 2-chlorobenzoate (**5**) was isolated as yellow oil and identified by GC-MS using the NIST Mass Spec. Data.¹²

Typical procedure by $\text{S}_{\text{RN}}1$ reactions photostimulated reactions of methyl 4-chlorobenzoate (**4**) with Me_3Sn^- ions in liquid ammonia

The following procedure is representative of these reactions. Me_3SnCl (1.2 mmol) and Na metal (2.4 mmol) were added to 250 mL of distilled ammonia. Na was added slowly in small pieces until total decoloration occurred. Then, 20 min after the last addition, when no more solid was present, the Me_3Sn^- ions were ready for use (a lemon yellow solution). Substrate **4** (1 mmol) was added to the solution and the reaction mixture irradiated for 1 h. The reaction was then quenched with an excess of ammonium nitrate, and the ammonia allowed to evaporate. The solid was dissolved in water, and HNO_3 was added to the water phase up to pH 7. The water phase was then extracted with chloroform (phase one), and HNO_3 was added to the water phase up to pH 3 before being extracted with chloroform (phase two). The products from chloroform phase one were isolated by Kügelrohr distillation. In the other experiments, the products were quantified by GLC using the internal standard method. The acid derivatizes from chloroform phase two were also quantified.

Dark reactions with Me_3Sn^- ions in liquid ammonia

This procedure was similar to that for the previous reaction, except that the reaction flask was wrapped with aluminium foil.

Inhibited reactions with Me_3Sn^- ions in liquid ammonia

This procedure was similar to that for the previous reaction, except that 10 mol% of either *p*-DNB or di-*tert*-butylnitroxide was added to the solution of nucleophile prior to substrate addition.

Isolation and identification of products

Methyl 4-chlorobenzoate (4**)**. This was isolated as a white solid after being extraction with diethyl ether–water. (EI+) *m/z* (%): 172 (10), 170 (30), 141 (9), 140 (9), 139 (100), 113 (13), 111 (36), 75 (26), 74 (8), 63 (1), 50 (11). Mp: 43–45 °C (lit.¹³ 43.5 °C).

Methyl 2-chlorobenzoate (5**)**. This was isolated as yellow oil after being extraction with diethyl ether–water. EM (EI+) *m/z* (%): 172 (10), 170 (28), 141 (33), 140 (8), 139 (100), 113 (11), 111 (32), 75 (25), 74 (7), 63 (1), 50 (11).

Methyl 4-(trimethylstanny)benzoate (7a**)**. This was isolated as amber liquid after Kügelrohr distillation (50 °C/1mmHg). (EI+) *m/z* (%): 289 (17), 287 (169), 286 (10), 285 (100), 284 (33), 283 (74), 282 (26), 281 (46), 255 (33), 254 (11), 253 (23), 252 (8), 251 (13). ¹H-NMR (400.16 MHz, CDCl_3) δ : 0.34 (9H, s, $J_{\text{H-Sn}} = 27.4$ Hz); 3.94 (3H, s); 7.50–7.70 (2H, d); 7.96–8.06 (2H, d). ¹³C-NMR (CDCl_3) δ : –9.5; 52.4; 128.4; 128.6; 129.8;

135.8; 149.6; 167.4. HRMS [MH]⁺ calc. for C₁₁H₁₇O₂Sn 301.0245, found: 301.0249.

Methyl 2-(trimethylstannyl)benzoate (7b). This was isolated as an amber liquid after Kügelrohr distillation (50 °C/1mmHg). (EI+) *m/z* (%): 289 (16), 287 (13), 286 (8), 285 (100), 284 (20), 283 (69), 282 (24), 281 (42), 255 (55), 254 (11), 253 (38), 251 (23). ¹H-NMR (400.16 MHz, CDCl₃) δ: 0.31 (9H, s, *J*_{H-Sn} = 27.4 Hz); 3.95 (3H, s); 7.40–7.48 (1H, t); 7.51–7.60 (1H, t); 7.64–7.80 (1H, d); 8.11–8.20 (1H, d); ¹³C-NMR (CDCl₃) δ: –7.4; 52.3; 128.3; 129.9; 131.9; 135.8; 136.5; 146.9; 168.9. HRMS [MH]⁺ calc. for C₁₁H₁₇O₂Sn 301.0245, found: 301.0236.

Methyl 3-(trimethylstannanyl)benzoate (7c). This was isolated as an amber liquid after Kügelrohr distillation (50 °C/1mmHg). EM (EI+) *m/z* (%): 289 (18), 287 (14), 286 (10), 285 (100), 284 (30), 283 (74), 282 (26), 281 (43), 255 (24), 254 (6), 253 (171), 251 (10). ¹H-NMR (400.16 MHz, CDCl₃) δ: 0.34 (9H, s, *J*_{H-Sn} = 27.4 Hz); 3.94 (3H, s); 7.39–7.45 (1H, t); 7.60–7.80 (1H, d); 7.95–8.05 (1H, d); 8.10–8.30 (1H, s); ¹³C-NMR (CDCl₃) δ: –9.4; 52.0; 127.8; 129.4; 129.5; 136.7; 140.3; 142.8; 167.5. HRMS [MH]⁺ calc. for C₁₁H₁₇O₂Sn 301.0245, found: 301.0253.

Methyl 5-chloro-2-(trimethylstannanyl)benzoate (3). This was isolated as a yellow oil after Kügelrohr distillation (50 °C/1mmHg). ¹H-NMR (CDCl₃) δ: 0.27 (9H, s, *J*_{H-Sn} = 27 Hz); 3.92 (3H, s); 7.49–7.61 (2H, m); 8.08–8.09 (1H, d). ¹³C-NMR (CDCl₃) δ: –7.4; 52.5; 129.8; 131.79; 137.7; 167.8. EM (EI+) *m/z* (%): 319 (100), 317 (73), 302 (4), 289 (50), 287 (36), 272 (3), 261(6), 259 (14), 231 (5), 165 (2), 151 (24), 133 (7), 118 (5), 89 (5), 75 (7), 63 (4). HRMS (CI) exact mass calc. for the C₁₁H₁₅ClO₂Sn (M⁺ – CH₃) 318.9548, found (M⁺ – CH₃) 318.9553.

Computational procedures

All calculations were carried out with DFT¹⁴ methods, as implemented in the Gaussian 03 package,¹⁵ by employing the B3LYP¹⁶ functional at the 6-31 + G* level of theory. This basis set is known to be appropriate for the theoretical study of the electronic and geometric properties of RAs.¹⁷ Stationary points were characterized by the normal analysis and obtained with complete geometry optimization without symmetry restrictions. Potential energy surfaces (PES) were obtained by varying the C–Cl bond length, and the B3LYP spin contamination along the whole fragmentation path was negligible (⟨S²⟩ = 0.750–0.751). The solvation effect was included by using a continuous model in acetonitrile solvent.

Acknowledgements

This work was supported in part by ACC, CONICET, SECYT and ANPCyT. J. P. M. and J. G. U. gratefully acknowledge receipt of fellowships from CONICET.

References

1 G. F. Smith, H. G. Kuivila, R. Simon and L. Sultan, *J. Am. Chem. Soc.*, 1981, **103**, 833–839; E. C. Ashby, W. Y. Su and T. N. Pham, *Organometallics*, 1985, **4**, 1493–1401; E. C. Ashby, R. N. DePriest

- and W. Y. Su, *Organometallics*, 1984, **3**, 1718–1727; J. San Filippo Jr. and J. Silbermann, *J. Am. Chem. Soc.*, 1981, **103**, 5588–5590.
- 2 R. A. Rossi, A. B. Pierini and A. B. Peñéñory, *Chem. Rev.*, 2003, **103**, 71–167; R. A. Rossi, A. B. Peñéñory, The Photo-stimulated S_{RN1} Process: Reaction of Haloarenes with Carbanions, in *CRC Handbook of Organic Photochemistry and Photobiology*, ed. W. M. Horspool and F. Lenel, CRC Press, Boca Raton, USA, 2nd edn, 2004, pp. 47; R. A. Rossi, Photoinduced Aromatic Nucleophilic Substitution Reactions, in *Synthetic Organic Photochemistry*, ed. A. G. Griesbeck and J. Mattay, Marcel Dekker, New York, 2005, pp. 495–527.
- 3 A. N. Santiago, S. M. Basso, J. P. Montañez and R. A. Rossi, *J. Phys. Org. Chem.*, 2006, **19**, 829–835.
- 4 S. M. Basso, J. P. Montañez and A. N. Santiago, *Lett. Org. Chem.*, 2008, **5**, 633–639.
- 5 R. K. Ingham, S. D. Rosenberg and H. Gilman, *Chem. Rev.*, 1960, **60**, 459–539.
- 6 The equation used in the relative reactivity determination of pairs of substrate vs. nucleophile was: $k_4/k_5 = \ln([\text{substrate } 4]_0/[\text{substrate } 4]_t)/\ln([\text{substrate } 5]_0/[\text{substrate } 5]_t)$, where [substrate 4]₀ and [substrate 5]₀ are initial concentrations and [substrate 4]_t and [substrate 5]_t are concentrations at time *t* of both substrates, see: J. F. Bunnett, in *Investigation of Rates and Mechanisms of Reactions*, ed. E. S. Lewis, Wiley-Interscience, New York, 3rd edn, 1974, part 1, pp. 159.
- 7 D. D. Tanner, J. J. Chen, L. Chen and C. Luelo, *J. Am. Chem. Soc.*, 1991, **113**, 8074–8881.
- 8 A. B. Pierini, J. S. Duca and M. A. Vera, *J. Chem. Soc., Perkin Trans. 2*, 1999, 1003–1009.
- 9 A. B. Pierini and J. S. Duca, *J. Chem. Soc., Perkin Trans. 2*, 1995, 1821–1828.
- 10 A. B. Pierini and D. M. A. Vera, *J. Org. Chem.*, 2003, **68**, 9191–9199.
- 11 D. M. Chipman, *J. Chem. Phys.*, 2000, **112**, 5558–5565; M. T. Cancas, B. Mennucci and J. Tomasi, *J. Chem. Phys.*, 1997, **107**, 3032–3041.
- 12 Mass Spectra, in *NIST Chemistry WebBook, NIST Standard Reference Database Number 69*, ed. P. J. Linstrom and W. G. Mallard, March 2003, National Institute of Standards and Technology, Gaithersburg MD, 20899, USA (<http://webbook.nist.gov>).
- 13 *CRC Handbook of Chemistry and Physics 78th edition*, CRC Press Inc., Boca Raton, USA, 1997.
- 14 W. Kohn and I. Sham, *Phys. Rev.*, 1965, **140**, A1133–A1138.
- 15 M. J. Frisch, G. W. Trucks, H. B. Schlegel, G. E. Scuseria, M. A. Robb, J. R. Cheeseman, J. A. Montgomery, Jr., T. Vreven, K. N. Kudin, J. C. Burant, J. M. Millam, S. S. Iyengar, J. Tomasi, V. Barone, B. Mennucci, M. Cossi, G. Scalmani, N. Rega, G. A. Petersson, H. Nakatsuji, M. Hada, M. Ehara, K. Toyota, R. Fukuda, J. Hasegawa, M. Ishida, T. Nakajima, Y. Honda, O. Kitao, H. Nakai, M. Klene, X. Li, J. E. Knox, H. P. Hratchian, J. B. Cross, V. Bakken, C. Adamo, J. Jaramillo, R. Gomperts, R. E. Stratmann, O. Yazyev, A. J. Austin, R. Cammi, C. Pomelli, J. Ochterski, P. Y. Ayala, K. Morokuma, G. A. Voth, P. Salvador, J. J. Dannenberg, V. G. Zakrzewski, S. Dapprich, A. D. Daniels, M. C. Strain, O. Farkas, D. K. Malick, A. D. Rabuck, K. Raghavachari, J. B. Foresman, J. V. Ortiz, Q. Cui, A. G. Baboul, S. Clifford, J. Cioslowski, B. B. Stefanov, G. Liu, A. Liashenko, P. Piskorz, I. Komaromi, R. L. Martin, D. J. Fox, T. Keith, M. A. Al-Laham, C. Y. Peng, A. Nanayakkara, M. Challacombe, P. M. W. Gill, B. G. Johnson, W. Chen, M. W. Wong, C. Gonzalez and J. A. Pople, *GAUSSIAN 03 (Revision B.02)*, Gaussian, Inc., Wallingford, CT, 2004.
- 16 C. Lee, W. Yang and R. G. Parr, *Phys. Rev. B: Condens. Matter*, 1988, **37**, 785–789; A. D. Becke, *Phys. Rev. A: At., Mol., Opt. Phys.*, 1988, **38**, 3098–3100; E. Miehlich, A. Savin, H. Stoll and H. Preuss, *Chem. Phys. Lett.*, 1989, **157**, 200–206.
- 17 D. M. A. Vera and A. B. Pierini, *Phys. Chem. Chem. Phys.*, 2004, **6**, 2899–2903; J. G. Uranga, D. M. A. Vera, A. N. Santiago and A. B. Pierini, *J. Org. Chem.*, 2006, **71**, 6596–6599.